

# Effective Shear Modulus of Honeycomb Cellular Structure

JOSEPH PENZIEN\*

*University of California, Berkeley, Calif*

AND

THEODOR DIDRIKSSON†

*Municipal Office of Reykjavik, Reykjavik, Iceland*

This paper examines the problem of theoretically predicting effective shear modulus of honeycomb core materials. Included in the analysis are the effects resulting from boundary conditions which prevent warpage of the cells. It is shown that these warpage constraints have little effect on shear modulus except when the ratio of core cell length to its lateral dimension becomes relatively small. A test procedure using a rigid shear frame is suggested for measuring effective shear modulus, and some test results obtained by this procedure are compared with the theoretical values.

## Nomenclature

$a, b$	= dimension of typical element of core shown in Fig 1
$d$	= thickness of the members of the shear loading frame (refer to Fig 8)
$E_\xi, E_\eta$	= moduli of elasticity of the core element $ABCD$ in the $\xi$ and $\eta$ directions, respectively [refer to Eqs (13) and (14)]
$E$	= $E_\eta$
$F$	= area of typical element of core as defined by Eq (2)
$f_1$	= $d/L_1$
$f_2$	= $d/L_2$
$G$	= shear modulus of the core material
$G$	= effective shear modulus of the honeycomb cellular material as defined by Eq (1) [refer also to Eq (53)]
$H$	= $\frac{1}{2}(a + b)$
$K_1, K_2$	= loading frame coefficients as defined by Eqs (46) and (52)
$K_3$	= quantity defined by Eq (50)
$L$	= depth of the core (refer to Fig 1)
$L_1, L_2$	= dimensions of the shear loading frame (refer to Fig 8)
$M_1, M_2, M_3, M_4$	= frictional moments developed at the joints of the shear loading frame (refer to Fig 8)
$P$	= diagonal loads applied to the shear loading frame (refer to Fig 8)
$p, q$	= shear flows in the typical core element induced by the shear forces $V_y$ and $V_x$ , respectively
$Q, Q'$	= shear forces between the core and the shear loading frame (refer to Fig 8)
$R$	= $b/a$
$r$	= radius of the shear loading frame holes
$S$	= dimensionless quantity defined by Eq (35)
$s$	= width of the core (refer to Fig 8)
$T$	= dimensionless quantity defined by Eq (36)
$t$	= thickness of the core material (refer to Fig 1)
$u, v$	= displacement components of the typical element $ABCD$ in the $\xi$ and $\eta$ directions, respectively [refer to Eqs (13) and (14)]
$V$	= shear force applied on the faces of the typical element of core (refer to Fig 2)

$V_x, V_y$	= components of $V$ in the $x$ and $y$ directions, respectively (refer to Figs 3 and 5)
$w$	= warpage parameter defined by Eq (10)
$\alpha$	= angle of inclination of the load $P$ applied to the shear loading frame (refer to Fig 8)
$\gamma$	= over-all shear strain of the typical element of the core
$\gamma_x, \gamma_y$	= components of $\gamma$ in the $x$ and $y$ directions, respectively
$\gamma_{\xi\eta}$	= shear strain in the element $ABCD$ [refer to Eq (15)]
$\gamma_1, \gamma_2$	= shear strains arising in the unrestrained typical element of the core under the shearing forces $V_x$ (refer to Fig 3b)
$\Delta$	= relative shear displacement vector of the typical element of core (refer to Fig 2)
$\Delta_x, \Delta_y$	= components of $\Delta$ in the $x$ and $y$ directions, respectively
$\epsilon_\xi, \epsilon_\eta$	= normal strain components of the typical element $ABCD$ in the $\xi$ and $\eta$ directions, respectively [refer to Eqs (13) and (14)]
$\theta$	= geometrical quantity of the typical core element (refer to Fig 1)
$\mu$	= coefficient of sliding friction between the pins and the shear loading frame
$\mu_\xi, \mu_\eta$	= Poisson's coefficients of the typical element $ABCD$ in the $\xi$ and $\eta$ directions, respectively [refer to Eqs (13) and (14)]
$\rho, \rho$	= densities of the core material and the core, respectively [refer to Eq (54)]
$\sigma_\xi, \sigma_\eta$	= normal stress components of the typical element $ABCD$ in the $\xi$ and $\eta$ directions, respectively
$\tau_{\xi\eta}$	= shearing stress in the typical element $ABCD$
$\phi, \psi$	= angles specifying the directions of the shear force $V$ and the relative shear displacement $\Delta$ , respectively (refer to Fig 2)

## Introduction

HONEYCOMB cellular materials are now widely used in the aircraft and missile industry because of their high strength-to-mass ratios. Usually these materials are bonded between flat or curved surfaces to form integral parts of load carrying structural elements.

Because of their characteristic geometry, honeycomb cellular materials are especially effective in transmitting shear loads. When carrying such loads, the amounts of shear deformation produced may be important design criteria; therefore, it is important that design engineers be able to predict these deformations analytically. To make these predictions, however, the effective shear moduli of these honeycomb cellular materials must be known. Although both analytical and experimental methods have been used

Received June 24, 1963; revision received November 26, 1963. The authors wish to express their appreciation and sincere thanks to those individuals who contributed to this investigation, and especially to Conway Chan, who designed the test frames and carried out the experimental tests, C. C. Tung, who reduced the final test data and checked the theoretical derivations, L. Umsted for typing this paper, and M. I. Kazimi of Hexcel Products, Inc. for his advice and encouragement. Finally, the authors wish to thank Hexcel Products, Inc. for their financial support which made this investigation possible.

\* Professor of Civil Engineering

† Structural Engineer

to predict effective shear moduli, considerable reluctance has been expressed by some engineers to accept these values as being sufficiently accurate. This reluctance is understandable when one observes the large variations in moduli that have been measured experimentally by several methods and poor correlations that appear to exist in some instances with theory.

It is the purpose of this report to set forth a sufficiently accurate theory for predicting effective shear moduli of honeycomb cellular materials and also to suggest an effective test procedure for measuring these quantities. A correlation of experimental results obtained by this suggested procedure with the theory presented herein is also included.

### Theoretical Analysis

The honeycomb cellular (or core) material analyzed in this report has a cross section as shown in Fig. 1. To determine the effective shear modulus of this material, consider the basic element of which it is made, as shown in Fig. 2. A shear force resultant  $V$  is applied to both the upper and lower faces of this element in opposite directions and at an angle  $\phi$  with the longitudinal  $x$  axis. The direction of the resulting relative shear displacement vector  $\Delta$  of the element does not, in general, coincide with the direction of the applied shear force. If one defines an angle  $\psi$  as the angle between the shear displacement vector  $\Delta$  and the longitudinal axis, then an effective shear modulus may be defined as

$$G \equiv V/F\gamma \cos(\phi - \psi) \quad (1)$$

where

$$F \equiv 2(b + a \cos \theta)a \sin \theta \quad (2)$$

is the rectangular area enclosing the typical element, and  $\gamma \equiv \Delta/L$  is the over-all shear strain of the element due to the applied shear force  $V$  ( $L$  being the depth of the core). It is evident from geometrical considerations that the component of the applied shear force in the transverse (longitudinal) direction does not produce shear displacement in the longitudinal (transverse) direction. Therefore, one may determine the relation between  $V_x$  and  $\gamma_x$  ( $\equiv \Delta_x/L$ ) and the relation between  $V_y$  and  $\gamma_y$  ( $\equiv \Delta_y/L$ ) separately. Here  $\Delta_x$  and  $\Delta_y$  represent the components of  $\Delta$  in the longitudinal and transverse directions, respectively; thus, the total shear strain  $\gamma$  is given by

$$(\gamma_x^2 + \gamma_y^2)^{1/2} \quad (3)$$

and the direction of the shear displacement by

$$\psi = \tan^{-1}(\gamma_y/\gamma_x) \quad (4)$$

To obtain the relation between  $V_x$  and  $\gamma_x$ , consider the typical element as shown in Fig. 3a, which is subjected to a uniform shear flow  $q$ . To satisfy the equilibrium condition in the vertical ( $z$ ) direction at each corner of the cell, the shear flow in each panel must, of course, be equal. Figure 3b

is an elevation view of the element showing the shear strain in each panel. It is readily seen that

$$\gamma_1 = q/Gt \quad (5)$$

$$\gamma_2 = \frac{qa(1 - \cos \theta)}{Gt(b + a \cos \theta)} \quad (6)$$

where  $G$  is the shear modulus of the core material. The over-all shear strain  $\gamma_z$  is

$$\gamma_z = \gamma_1 + \gamma_2 = \frac{q}{Gt} \frac{2H}{a(R + \cos \theta)} \quad (7)$$

where

$$R = b/a \quad (8)$$

$$H = (a + b)/2 \quad (9)$$

Under this loading condition, it is apparent that warping occurs at the upper and lower faces of the core element. The warpage parameter  $w$  is defined as

$$w \equiv \left(\frac{b}{2}\right) \gamma_2 = \frac{qb(1 - \cos \theta)}{2GT(R + \cos \theta)} \quad (10)$$

However, in most practical cases, as well as in the experiment that will be described in the subsequent section, the faces of the core are constrained so that they remain essentially plane during deformation; that is, the actual configuration of the deformed core element is as shown by the dashed lines in Fig. 3b.

To study the effect that the constraint against warpage of the faces has on the shear modulus of the core, consider the element  $ABCD$  in Fig. 3b. One must now find the corrective state of stress in this element when subjected to the displacement boundary conditions that the vertical edges  $AD$  and  $BC$  are simply supported, and the upper and lower edges  $AB$  and  $CD$  are subjected to vertical displacements equal in magnitude but opposite in direction to the warpage indicated in Fig. 3b. Several simplifications and assumptions are made in the following analysis. First, the inclined panel I is unfolded into the plane of panel II. Second, it is assumed that the amount of stretching of the panels in the direction perpendicular to the direction of the essential normal stresses is negligible. Consequently, one may consider the panels as composed of an orthotropic material that is rigid in one direction. Third, the thickness  $t$  of the panels is so small compared with other dimensions that one can consider the state of stress in the panels as being plane stress. The typical element  $ABCD$  is again shown in Fig. 4. The equations of equilibrium for element  $ABCD$  are given by

$$(\partial \sigma_\xi / \partial \xi) + (\partial \tau_{\xi\eta} / \partial \eta) = 0 \quad (11)$$

$$(\partial \tau_{\xi\eta} / \partial \xi) + (\partial \sigma_\eta / \partial \eta) = 0 \quad (12)$$

The stress-strain relationships are

$$\epsilon_\xi = (\partial u / \partial \xi) = (\sigma_\xi - \mu_\xi \eta_\eta) / E_\xi \quad (13)$$

$$\epsilon_\eta = (\partial u / \partial \eta) = (\sigma_\eta - \mu_\eta \sigma_\xi) / E_\eta \quad (14)$$

$$\gamma_{\xi\eta} = (\partial u / \partial \eta) + (\partial v / \partial \xi) = (1/G) \tau_{\xi\eta} \quad (15)$$

In these equations,  $\sigma_\xi$ ,  $\sigma_\eta$ ,  $\tau_{\xi\eta}$  and  $\epsilon_\xi$ ,  $\epsilon_\eta$ ,  $\gamma_{\xi\eta}$  are the stress and

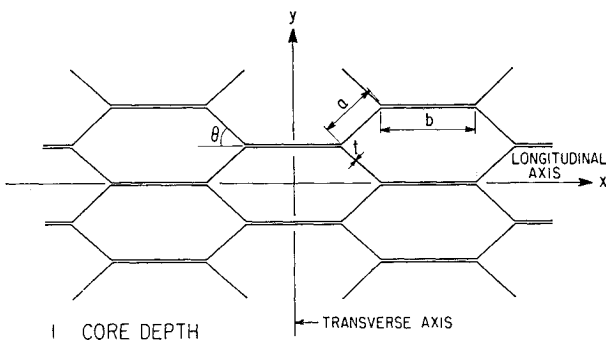


Fig. 1 Geometry of honeycomb cells

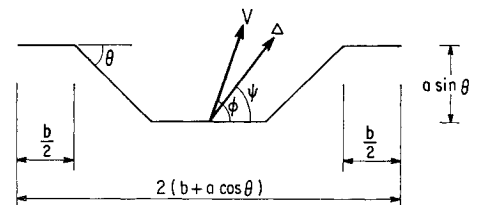


Fig. 2 Typical element of the core

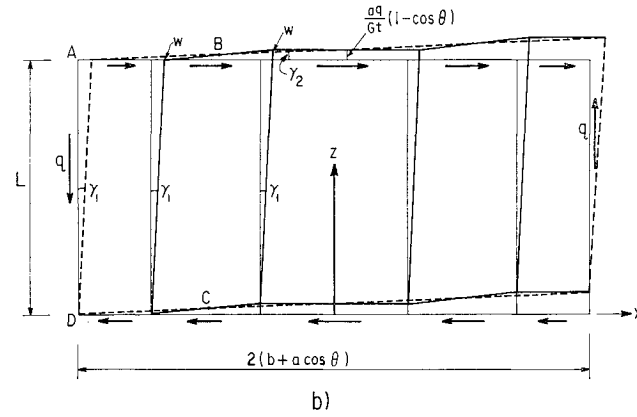
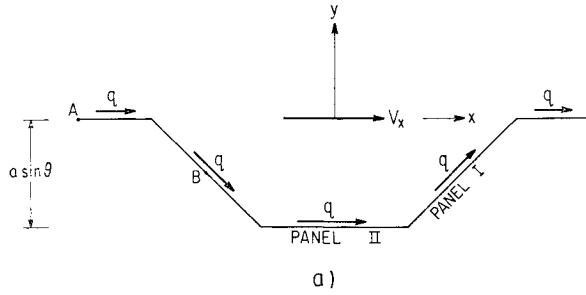


Fig 3 Shear strains in core element

strain components, respectively, and  $u, v$  are the displacement components in the  $\xi$  and  $\eta$  directions, respectively. The terms  $E_\xi, E_\eta$  and  $\mu_\xi, \mu_\eta$  are the moduli of elasticity and Poisson's ratios of the core material in the  $\xi$  and  $\eta$  directions, respectively. For a plate that is rigid in one direction,

$$E_\xi = \infty \quad (16)$$

$$\mu_\eta = 0 \quad (17)$$

Thus, Eq (13) becomes

$$\partial u / \partial \xi = 0 \quad (18)$$

and  $u$  is a function of the variable  $\eta$  only; that is,  $u = u(\eta)$

If  $E$  is written for  $E_\eta$ , Eqs (14) and (15) take the form

$$E(\partial v / \partial \eta) = \sigma_\eta \quad (19)$$

$$G(\partial v / \partial \xi) = \tau_{\xi\eta} - u'(\eta)G \quad (20)$$

Differentiating Eqs (19) and (20) with respect to  $\eta$  and  $\xi$ , respectively, and substituting into Eq (12), one obtains

$$G(\partial^2 v / \partial \xi^2) + E(\partial^2 v / \partial \eta^2) = 0 \quad (21)$$

The boundary conditions are

$$v(0, \eta) = v(H, \eta) = 0$$

$$v(\xi, 0) = v(\xi, L) = \begin{cases} (2w/b)\xi & 0 \leq \xi \leq b/2 \\ (2w/a)(H - \xi) & b/2 \leq \xi \leq H \end{cases} \quad (22)$$

The solution of the partial differential Eq (21) with boundary conditions (22) may be obtained by Fourier's method. The final solution, which results by this method, is

$$v = \sum_{n=1}^{\infty} \beta_n \sin \frac{n\pi}{H} \xi \frac{1}{\sinh g_n L} [\sinh g_n(L - \eta) + \sinh g_n \eta] \quad (23)$$

where

$$g_n^2 = \frac{G}{E} \left( \frac{n\pi}{H} \right)^2 = \frac{1}{2(1 + \mu_\eta)} \left( \frac{n\pi}{H} \right)^2 \quad (24)$$

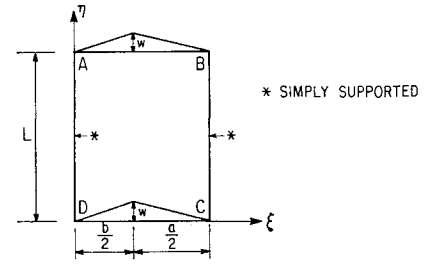


Fig 4 Typical element ABCD

and

$$\beta_n = \frac{2}{H} \left[ \int_0^{b/2} \frac{2w}{b} \xi \sin \frac{n\pi}{H} \xi d\xi + \int_{b/2}^H \frac{2w}{a} (H - \xi) \sin \frac{n\pi}{H} \xi d\xi \right] \quad (25)$$

Substituting Eq (10) into Eq (25) and integrating, one obtains

$$\beta_n = \frac{4q}{Gta} \frac{(1 - \cos \theta)}{(R + \cos \theta)} \frac{\sin \{n\pi[R/(1 + R)]\}}{(n\pi/H)^2} \quad (26)$$

The normal stresses in the panels may now be obtained from Eq (19); thus

$$\sigma_n = E \frac{\partial v}{\partial \eta} = E \sum_{n=1}^{\infty} \frac{\beta_n g_n \sin[(n\pi/H)\xi]}{\sinh g_n L} \times [\cosh g_n \eta - \cosh g_n(L - \eta)] \quad (27)$$

The shear stresses are similarly obtained from Eq (20). Equation (18) shows that  $u$  is independent of  $\xi$ ; that is,  $u = u(\eta)$ , and therefore, since  $u(\eta) = 0$  at both  $\xi = 0$  and  $\xi = H$ ,  $u(\eta) = 0$  throughout the panel. Hence, Eq (20) gives

$$\tau_{\xi\eta} = G \frac{\partial v}{\partial \xi} = G \sum_{n=1}^{\infty} \frac{\beta_n (n\pi/H) \cos[(n\pi/H)\xi]}{\sinh g_n L} \times [\sinh g_n(L - \eta) + \sinh g_n \eta] \quad (28)$$

The total shear stresses and the normal stresses in the unwarped deformed element ABCD in Fig 3b are

$$\tau = (q/t) + \tau_{\xi\eta} \quad (29)$$

$$\sigma = \sigma_\eta \quad (30)$$

The corresponding shear forces  $V_x$  may now be evaluated by energy considerations. The total external work is

$$\text{external work} = (\gamma_x L V_x) / 8 \quad (31)$$

where  $\gamma_x$  is the over-all shear strain given by Eq (7). The total strain energy is

$$\text{strain energy} = \int \frac{\tau^2}{2G} d\gamma + \int \frac{\sigma^2}{2E} d\gamma \quad (32)$$

where  $d\gamma$  is the differential volume of the element under consideration, and the integration extends over the entire volume of the element ABCD. Substitution of Eqs (7) and (27-30) into the energy equation

$$\frac{1}{2} \gamma_x L \frac{V_x}{4} = \int \frac{\tau^2}{2G} d\gamma + \int \frac{\sigma^2}{2E} d\gamma \quad (33)$$

gives, after integrating and rearranging the following expression for the shear  $V_x$ ,

$$V_x = 2qa(R + \cos \theta)(1 + ST) \quad (34)$$

where

$$S = \frac{2(1 - \cos \theta)^2(1 + R)^2[2(1 + \mu_\eta)]^{1/2}}{(L/H)\pi^2(R + \cos \theta)^2} \quad (35)$$

$$T = \sum_{n=1}^{\infty} \frac{1}{n^2} \left\{ \frac{\sin[n\pi R/(1+R)]}{\sinh g_n L} \right\}^2 \times (\sinh 2g_n L - 2 \sinh g_n L) \quad (36)$$

Eliminating  $q$  from Eqs (7) and (34) gives

$$\gamma_x = \frac{HV \cos \phi}{Gt a^2 (R + \cos \theta)^2 (1 + ST)} \quad (37)$$

where  $V \cos \phi = V_x$ . The term  $ST$  is due to the prevention of warpage

To determine the relation between  $V_y$  and  $\gamma_y$ , consider the typical element acted upon by the shear flows  $p$  as indicated in Fig 5. It is evident from geometrical considerations that there will be no warping. The over-all shear strain is

$$\gamma_y = p/(Gt \sin \theta) \quad (38)$$

and the shear force  $V_y$  is

$$V_y = 2pa \sin \theta \quad (39)$$

Eliminating  $p$  from Eqs (38) and (39) gives the following relation between  $\gamma_y$  and  $V_y$ :

$$\gamma_y = (V \sin \phi)/(2aGt \sin^2 \theta) \quad (40)$$

where

$$V \sin \phi = V_y$$

The effect of preventing warpage upon the value of the shear modulus of the core is now studied for the particular case where  $\phi = 0$ ,  $R = 1$ ,  $\theta = 60^\circ$ , and  $\mu_n = 0.33$ . The final result of this study is shown in Fig 6. It is seen that for moderately large values of  $L/H$  the effect of the prevention of warpage may be ignored. In such cases, Eq (37) reduces to

$$\gamma_x = \frac{HV \cos \phi}{Gta^2(R + \cos \theta)^2} \quad (41)$$

Equation (41) together with Eq (40) gives

$$\gamma = \frac{V}{Gta} \left[ \frac{H^2 \cos^2 \phi}{a^2(R + \cos \theta)^4} + \frac{\sin^2 \phi}{4 \sin^4 \theta} \right]^{1/2} \quad (42)$$

$$\cos(\phi - \psi) = \left[ \frac{\sin^2 \phi}{2 \sin^2 \theta} + \frac{H \cos^2 \phi}{a(R + \cos \theta)^2} \right] \times \left[ \frac{H^2 \cos^2 \phi}{a^2(R + \cos \theta)^4} + \frac{\sin^2 \phi}{4 \sin^4 \theta} \right]^{-1/2} \quad (43)$$

Substitution of these expressions into Eq (1) gives

$$\frac{G_e}{G} = \frac{\sin \theta (R + \cos \theta)}{a/t[(1+R) \sin^2 \theta \cos^2 \phi + (R + \cos \theta)^2 \sin^2 \phi]} \quad (44)$$

### Experimental Investigation

To induce pure shear in a core, a rigid frame pinned at the four corners, as shown in Fig 7, was designed within which honeycomb core is bonded on four sides. Essentially pure shear deformation of the core specimen results when the tensile loads  $P$  are applied with their lines of action passing through two diagonally opposite pins. The relative dis-

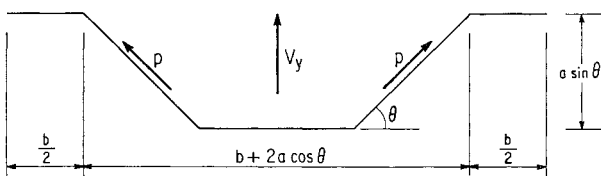


Fig 5 Plan view of typical element of the core

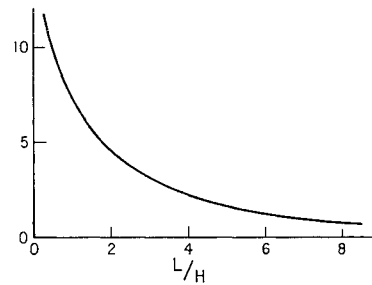


Fig 6 Percentage increase of the effective shear modulus ratio  $G_e/G$  due to the prevention of warpage vs  $L/H$

placements  $\Delta$  of the upper and lower faces of the frame were measured by a transducer attached to the lower member of the frame and a rod rigidly attached to the upper member and extended down to the transducer. During the test program, the load  $P$  and its corresponding displacement  $\Delta$  were recorded graphically as the load increased. Tests were performed on Hexcel Honeycomb cores made of 0.0007-in-thick aluminum alloy (5052-H39) foil. The core size, i.e.,  $2a \sin \theta$ , was equal to  $\frac{1}{8}$  in. For this particular core material  $a = b$ . All specimens were loaded in the longitudinal direction as shown in Fig 1.

To deduce effective shear modulus of a core from test results, consider the loading frame shown in Fig 8. Acting on the frame are the externally applied forces  $P$  and the interacting shear forces  $Q$  and  $Q'$  between the core and the frame where  $Q' = Q(L_2 - d)/(L_1 - d)$  to satisfy equilibrium conditions of the core. The relation between the shear force  $Q$  and the applied force  $P$  can be deduced easily by applying the principle of virtual work to the equilibrium conditions of the frame. If frictionless pins are assumed, i.e.,  $M_1 = M_2 = M_3 = M_4 = 0$ , one obtains

$$Q = K_1 P \cos \alpha \quad (45)$$

where

$$K_1 \equiv (1 - f_1)/(1 - f_1 f_2) \quad f_1 \equiv d/L_1 \quad f_2 \equiv d/L_2 \quad (46)$$

During the tests, however, tangential frictional forces are developed on the pins because of their rotational slippage (or impending slippage) with respect to the frame. To determine the effects of these frictional forces on the relation between shear force  $Q$  and applied force  $P$ , a static analysis of the frame is first made assuming frictionless pins. This analysis yields the normal forces that are exerted on each of the four members of the frame by the pins. It will be noted that the pin forces at joints  $A_1$  and  $A_3$  are small compared to those at joints  $A_2$  and  $A_4$  where the forces  $P$  are applied; therefore, one needs to consider only those tangential frictional forces developed at joints  $A_2$  and  $A_4$ . Letting  $F_1$  and  $F_2$  designate the normal forces that pin  $A_2$  exerts on members  $A_1A_2$  and  $A_2A_3$ , respectively, and letting  $F_3$  and  $F_4$  designate the normal forces that pin  $A_4$  exerts on members  $A_3A_4$  and  $A_1A_4$ , respectively, the foregoing static analysis gives

$$F_1 = F_3 = \frac{1}{2}(1 + K_1)P \cos \alpha \quad (47)$$

$$F_2 = F_4 = (L_2/2L_1)(1 + K_3)P \cos \alpha \quad (48)$$

where

$$K_3 \equiv (1 - f_2)/(1 - f_1 f_2) \quad (49)$$

Correspondingly, letting  $M_1$  and  $M_2$  designate the maximum moments that could be developed by pin  $A_2$  upon members  $A_1A_2$  and  $A_2A_3$ , respectively, and letting  $M_3$  and  $M_4$  designate the maximum moments that could be developed by pin  $A_4$  upon members  $A_3A_4$  and  $A_1A_4$ , respectively (assuming rotational slippage to occur in each case), the following relations result:

$$M_1 = M_3 \cong F_1 \mu r = (\mu r/2)(1 + K_1)P \cos \alpha \quad (50)$$

$$M_2 = M_4 \cong F_2 \mu r = (\mu r/2)(L_2/L_1)(1 + K_3)P \cos \alpha \quad (51)$$

where  $r$  is the radius of the frame holes, and  $\mu$  is the coefficient of sliding friction between the pins and the frame. The moments given by Eqs (50) and (51) are only approximate, since it has been assumed that the existence of these moments do not influence the magnitude of the pin forces as given by Eqs (47) and (48). Little loss of accuracy results, however, from this assumption.

At this point in the analysis, one must recognize that, to maintain rotational equilibrium of pins  $A_2$  and  $A_4$ ,  $M_1 = M_2$  and  $M_3 = M_4$ . With  $L_1$  selected as the larger of the two frame dimensions  $L_1$  and  $L_2$ , moments  $M_2$  and  $M_4$  as given by Eq (51) are smaller than moments  $M_1$  and  $M_3$  as given by Eq (50); thus, pins  $A_2$  and  $A_4$  will first slip with respect to members  $A_2A_3$  and  $A_1A_4$ , respectively, when moments  $M_2$  and  $M_4$  reach the intensity given by Eq (51). These same pins will therefore not slip with respect to members  $A_1A_2$  and  $A_3A_4$ , since  $M_1$  and  $M_3$  must be limited to the value of  $M_2$  and  $M_4$  as given by Eq (51).

A relation between the shear force  $Q$  and the applied force  $P$ , which includes the effects of pin friction, can now be deduced by again applying the principle of virtual work to the equilibrium conditions of the frame. Since slippage of pins  $A_2$  and  $A_4$  occur with respect to members  $A_2A_3$  and  $A_1A_4$  only, moments  $M_2$  and  $M_4$  contribute to the total virtual work done on the frame, but  $M_1$  and  $M_3$  do not contribute. This analysis leads to the expression

$$Q = K_2 P \cos \alpha \quad (52)$$

where

$$K_2 \equiv K_1 \{1 - (\mu r/L_1)(1 + K_3)\} \quad (53)$$

If the pins and frame holes are well lubricated so that the coefficient of friction  $\mu$  is minimized, then  $K_2$  can be approximated with sufficient accuracy by  $K_1$ .

The measured effective shear moduli of the cores are deduced from the experimental data by the expression

$$G_c = \frac{Q}{s\Delta} \left( \frac{L_2 - d}{L_1 - d} \right) = \frac{PK_1 \cos \alpha}{s\Delta} \left( \frac{1 - f_2}{1 - f_1} \right) \frac{f_1}{f_2} \quad (54)$$

where  $s$  is the width of the core measured normal to the view of the frame as shown in Fig 8, and  $i$  assumes a value of one or two depending upon whether or not pin friction is to be included.

### Comparison of Experimental and Theoretical Shear Moduli

Since all tests were performed on cores whose depths  $L$ , compared to the lateral dimensions  $H$  of the cells, are large,

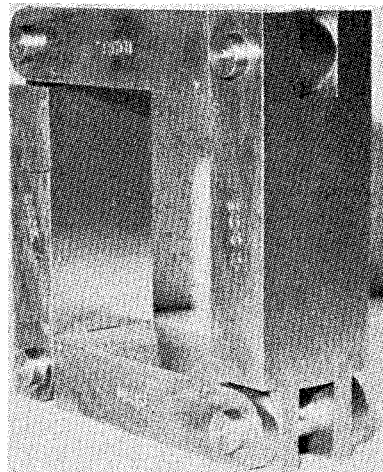


Fig 7 Test frame

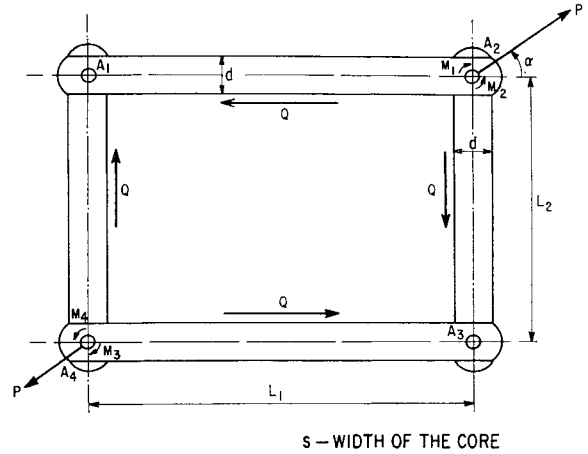


Fig 8 Shear loading frame

the effect of warpage may be neglected and Eq (44) may be used for the determination of the theoretical shear moduli of the cores. Introducing now the density of the honeycomb

$$\rho = \frac{(1 + R)\rho_c}{(a/t)(R + \cos \theta) \sin \theta} \quad (55)$$

where  $\rho_c$  and  $\rho$  are the densities of the core and the foil material, respectively, Eq (44) reduces to

$$\frac{G_c}{G} \frac{\rho}{\rho_c} = \frac{(R + \cos \theta)^2 \sin^2 \theta}{(1 + R)[(1 + R) \sin^2 \theta \cos^2 \phi + (R + \cos \theta)^2 \sin^2 \phi]} \quad (56)$$

Since, in the experiments, the load  $P$  was applied in the longitudinal direction, i.e.,  $\phi = 0$ , Eq (56) becomes

$$\frac{G_c}{G} \frac{\rho}{\rho_c} = \frac{(R + \cos \theta)^2}{(1 + R)^2} \quad (57)$$

Using Eqs (54) and (57), it is found that the ratio of the experimental effective shear moduli of the cores to their respective theoretical values ranges approximately from 1.04 to 1.10 when the effect of friction forces at the joints are not taken into consideration. When the friction forces are considered and a value  $\mu = 0.25$  is used, this same ratio ranges from 1.04 to 1.06.

### Conclusions

Based on the results of this investigation, the following general conclusions have been deduced:

1) The effective shear modulus of typical honeycomb cores can be determined with sufficient accuracy for design purposes using the theory presented in this report.

2) The prevention of warpage of the core cross section has only a small effect on the effective shear modulus when the ratio of the depth of core  $L$  to the lateral dimension  $H$  of the cell is large [e.g., a 1% change results when  $L/R$  is approximately 7 (see Fig 6)].

3) The effective shear modulus of honeycomb cores can be measured effectively using the "shear frame" test described herein. The variations in moduli measured for a given core material by this method are within a range which would be expected as a result of the variations in the geometrical quantities from one sample to another and the variations in the shear moduli of the core material itself.